Clinical Cancer Research

PARP Inhibitor Upregulates PD-L1 Expression and Enhances Cancer-Associated Immunosuppression

Shiping Jiao[1,2], Weiya Xia[1], Hirohito Yamaguchi[1], Yongkun Wei[1], Mei-Kuang Chen[1,2], Jung-Mao Hsu[1], Jennifer L. Hsu[1,3,4], Wen-Hsuan Yu[1,2], Yi Du[1], Heng-Huan Lee[1], Chia-Wei Li[1], Chao-Kai Chou[1], Seung-Oe Lim[1], Shih-Shin Chang[1], Jennifer Litton[5], Banu Arun[5], Gabriel N. Hortobagyi[5], and Mien-Chie Hung[1,2,3,4]

Abstract

Purpose: To explore whether a cross-talk exists between PARP inhibition and PD-L1/PD-1 immune checkpoint axis, and determine whether blockade of PD-L1/PD-1 potentiates PARP inhibitor (PARPi) in tumor suppression.

Experimental Design: Breast cancer cell lines, xenograft tumors, and syngeneic tumors treated with PARPi were assessed for PD-L1 expression by immunoblotting, IHC, and FACS analyses. The phospho-kinase antibody array screen was used to explore the underlying mechanism of PARPi-induced PD-L1 upregulation. The therapeutic efficacy of PARPi alone, PD-L1 blockade alone, or their combination was tested in a syngeneic tumor model. The tumor-infiltrating lymphocytes and tumor cells isolated from syngeneic tumors were analyzed by CyTOF and FACS to evaluate the activity of antitumor immunity in the tumor microenvironment.

Results: PARPi upregulated PD-L1 expression in breast cancer cell lines and animal models. Mechanistically, PARPi inactivated GSK3β, which in turn enhanced PARPi-mediated PD-L1 upregulation. PARPi attenuated anticancer immunity via upregulation of PD-L1, and blockade of PD-L1 resensitized PARPi-treated cancer cells to T-cell killing. The combination of PARPi and anti-PD-L1 therapy compared with each agent alone significantly increased the therapeutic efficacy *in vivo*.

Conclusions: Our study demonstrates a cross-talk between PARPi and tumor-associated immunosuppression and provides evidence to support the combination of PARPi and PD-L1 or PD-1 immune checkpoint blockade as a potential therapeutic approach to treat breast cancer. *Clin Cancer Res; 23(14); 3711–20.* ©2017 AACR.

Introduction

PARP engages in DNA base excision repair by inducing poly (ADP-ribosy)lation of itself and other target proteins (1). PARP inhibition has been shown to be an effective therapeutic strategy against tumors associated with germline mutation in double-strand DNA repair genes by inducing synthetic lethality (1). One PARP inhibitor (PARPi), olaparib, was approved by the FDA in 2014 for the treatment of germline *BRCA*-mutated (gBRCAm) advanced ovarian cancer (2). More recently, another PARPi, niraparib, which was shown to significantly prolong the progression-free survival in ovarian cancer patients, received a fast track designation from the FDA for the treatment of patients with recurrent platinum-sensitive ovarian cancer (3).

In addition to ovarian cancer, PARPi has demonstrated tremendous potential in breast cancer, and there are currently several active clinical trials evaluating PARPi-containing combination therapies for advanced breast cancer. For instance, several combinations of PARPi and targeted anticancer agents, such as inhibitors against PI3K (4, 5), Wee1 kinase (6), DNA topoisomerase I (7), and DNA methyltransferase (8), have been proposed to enhance the cytotoxic effect of PARPi. In addition, c-Met–mediated phosphorylation of PARP was reported to contribute to PARPi resistance, suggesting that the combined inhibition of c-Met and PARP may benefit patients who do not respond to PARPi and whose tumors are associated with c-Met activation (9). Thus, developing a rational combination therapy with PARPi may lead to effective anticancer strategy.

Over the past few years, there have been major breakthroughs in our understanding of tumor-associated immunosuppression. A key mechanism underlying cancer immune evasion is the expression of multiple inhibitory ligands, notably PD-L1, on the surface of cancer cells. Engagement of the PD-1 receptor on T cells by PD-L1 leads to the suppression of T-cell proliferation, cytokine release, and cytolytic activity, whereas blockade of coinhibitory ligation with mAbs, such as PD-L1 or PD-1 antibodies, restores T-cell function and increases therapeutic efficacy (10, 11). The impressive and durable clinical response of checkpoint blockade immunotherapy resulted in the FDA approval of ipilimumab, nivolumab, pembrolizumab, and more recently atezolizumab for the treatment of multiple types of cancer, such as melanoma,

[1]Department of Molecular and Cellular Oncology, The University of Texas MD Anderson Cancer Center, Houston, Texas. [2]The University of Texas Graduate School of Biomedical Sciences at Houston, Houston, Texas. [3]Graduate Institute of Biomedical Sciences and Center for Molecular Medicine, China Medical Univesity, Taichung, Taiwan. [4]Department of Biotechnology, Asia University, Taichung, Taiwan. [5]Department of Breast Medical Oncology, The University of Texas MD Anderson Cancer Center, Houston, Texas.

Note: Supplementary data for this article are available at Clinical Cancer Research Online (http://clincancerres.aacrjournals.org/).

Corresponding Author: Mien-Chie Hung, Department of Molecular and Cellular Oncology, The University of Texas MD Anderson Cancer Center, 1515 Holcombe Blvd. Unit 108, Houston, TX 77030. Phone: 713-792-3668; Fax: 713-794-3270; E-mail: mhung@mdanderson.org

doi: 10.1158/1078-0432.CCR-16-3215

Translational Relevance

With the recent approval of therapeutic antibodies that block CTLA4, PD-1, and PD-L1, immune checkpoints have emerged as new targets in cancer therapy. In addition, there is accumulating evidence highlighting the role of cancer-associated immunity in patient response to cytotoxic anticancer agents. Inhibitors of PARP have shown substantial cytotoxic effects against tumors with defects in DNA damage response. However, whether a cross-talk between PARP inhibition and immune checkpoints exists remains unclear. Here, we show that PARP inhibitor (PARPi) treatment upregulates tumor cell PD-L1 expression, which attenuates PARPi efficacy via cancer-associated immunosuppression. The blockade of PD-L1 can restore the attenuated antitumor immunity and potentiate PARPi in tumor suppression. This study provides a scientific rationale for the evaluation of PD-L1/PD-1 blockade with PARPi in clinical trials.

Hodgkin lymphoma, and lung and bladder cancers (12–15). Notably, the PD-1 antibody pembrolizumab was approved as first-line treatment for patients with advanced non–small cell lung cancer and high PD-L1 expression (16).

There is accumulating evidence indicating that conventional and targeted anticancer therapies also affect tumor-targeting immune responses (17). Thus, delineating the cross-talk between cytotoxic anticancer agents and cancer-associated immunity may lead to more efficient combinatorial regimens. Although the effects of PARPi, a targeted anticancer agent, have shown promising results in multiple cancer types, how and whether PARPi plays a role in cancer-associated immunity is still unknown. In the current study, we investigate the cross-talk between PARP inhibition and immune checkpoint, in particular, the PD-L1/PD-1 axis, which is a dominant immune checkpoint pathway in the tumor microenvironment, and further explore a mechanism-driven combination strategy to potentiate PARPi.

Materials and Methods

Cell lines

All cell lines were obtained from ATCC and have been independently validated by STR DNA fingerprinting at MD Anderson Cancer Center (Houston, TX). PARP1 (#sc-400046), PD-L1 (#sc-401140), and GSK3β (#sc-425249) knockout cells were established using CRISPR/Cas9 KO plasmids from Santa Cruz Biotechnology. PARP1 knockdown MDA-MB-231 cells were established as described previously (9).

Antibodies and chemicals

PD-L1 (#13684), PARP1 (#9532), phospho-GSK3β (Ser9, #9336), GSK3β (#9315), and Ki-67 (#9449) antibodies were purchased from Cell Signaling Technology, BRCA1 (sc-8326) and BRCA2 (sc-642) were from Santa Cruz Biotechnology, and α-tubulin (#B-5-1-2) and β-actin (#A2228) were obtained from Sigma-Aldrich. Olaparib, rucaparib, and talazoparib were purchased from Selleckchem, ChemieTek, and Selleckchem, respectively. Human CD274 (B7-H1, PD-L1) antibody for T-cell killing assay was from BioLegend (#329709). eSiRNA human BRCA1 (EHU096311), eSiRNA human BRCA2 (EHU031451), and siRNA universal negative control (SIC001) were from Sigma-Aldrich.

Human phospho-kinase antibody array

The Human Phospho-Kinase Array Kit (#ARY003B) was purchased from R&D Systems. Array screening was performed following the manufacturer's protocol. Briefly, cell lysates were incubated with the array membranes. After washing, the membranes were incubated with biotinylated antibody cocktail. The amounts of phospho-kinase were assessed with streptavidin conjugated to horseradish peroxidase (HRP), followed by chemiluminescence detection. A GS-800 Calibrated Densitometer (Bio-Rad Laboratories) was used to quantify the density of each dot against the average of the internal controls on the membrane as indicated in the protocol.

Detection of cell surface PD-L1

For detection of cell surface PD-L1, cells were suspended in 100 μL of cell staining buffer (#420201, BioLegend) and incubated with APC-conjugated anti-human PD-L1 antibody (#329708, BioLegend) at room temperature for 30 minutes. After washing in the staining buffer, stained cells were analyzed by FACS (BD Biosciences).

PD-L1/PD-1–binding assay

Cells (1×10^6) were incubated with 5 μg/mL recombinant human PD-1 FC chimera protein (#1086-PD-050, R&D Systems) at room temperature for 30 minutes. After washing in staining buffer, cells were incubated with anti-human Alexa Fluor 488 dye conjugated antibody (Thermo Fisher Scientific) at room temperature for 30 minutes. Cells were analyzed by FACS after wash in the staining buffer. The FACS data were analyzed using FlowJo (Tree Star), and the cut-off line for relative positive percentage was set at the median of the maximum signal.

T-cell killing assay

NucLight RFP MDA-MB-231 cells (#4457, Essen Bioscience) were seeded in a 96-well plate with or without olaparib. Human peripheral blood mononuclear cells (PBMC; #70025, STEMCELL) were activated with 100 ng/mL CD3 antibody, 100 ng/mL CD28 antibody, and 10 ng/mL IL2 (#317303; #302913; #589102, BioLegend) and then cocultured with MDA-MB-231 cells at 10:1 ratio in the presence of fluorescence caspase-3/7 substrate (#4440, Essen Bioscience).

PD-L1 detection in xenograft tumors

All animal procedures were conducted under the guidelines approved by the Institutional Animal Care and Use Committee at UT MD Anderson Cancer Center. MDA-MB-231 (0.5×10^6), BT549 (1×10^6), or SUM149 (2×10^6) cells in Matrigel (BD Biosciences) were injected into the mammary fat pads of female nude mice of 6 to 8 weeks of age. When tumor volume reached approximately 50 mm^3, mice were administered olaparib (25 mg/kg) or rucaparib (5 mg/kg) orally 5 days per week for 3 weeks. Tumors were collected after final treatment and analyzed by immunoblotting and IHC. IHC staining was performed as described previously (18). Briefly, frozen tissue sections were fixed with 4% paraformaldehyde for 1 hour and then hydrated in PBS for 5 minutes at room temperature. Sections were permeabilized with 0.5% Triton X-100 for 15 minutes at room temperature. The

endogenous peroxidase activity was blocked with 0.3% hydrogen peroxide in methanol for 15 minutes at room temperature. After serum blocking, the slides were incubated overnight at 4°C with human PD-L1 antibody (#13684, Cell Signaling Technology, 1:50 dilution). Slides were then incubated with biotinylated secondary antibodies for 1 hour at room temperature, followed by incubation with avidin–biotin–HRP complex. Visualization was performed using 0.125% amino-ethylcarbazole chromogen. After counterstaining with Mayer's hematoxylin, slides were mounted.

Syngeneic tumor model treatment protocol

BALB/c mice (6- to 8-week-old female, The Jackson Laboratory) were inoculated in the mammary fat pads with EMT6 (1×10^5) cells in Matrigel. On days 3 after the inoculation, mice were injected intraperitoneally with 50 mg/kg olaparib or vehicle daily. After day 4, mice were injected intraperitoneally every 4 days with 75 μg anti-mouse PD-L1 antibody (10F.9G2, Bio X Cell) or control rat IgG2b (LTF-2, Bio X Cell). Tumor volumes were measured every 3 days with a digital caliper and were calculated using the formula: $\pi/6 \times \text{length} \times \text{width}^2$. Body weight was measured every 5 days.

Tumor cell PD-L1 expression and tumor-infiltrating lymphocyte analysis

EMT6 tumors were excised and digested in collagenase/hyaluronidase and DNase I and dissociated by gentleMACS Dissociator as described by the protocol of Tumor Dissociation Kit (Miltenyi Biotec). Tumor cells and tumor-infiltrating lymphocytes (TIL) were enriched and harvested separately by Percoll gradient (Sigma). Cell surface PD-L1 of tumor cell were stained with Brilliant Violet 421–conjugated anti-mouse PD-L1 antibody (#124315, BioLegend) and analyzed by FACS, and TILs were stained and analyzed by mass cytometry (CyTOF). The antibodies used to stain TILs are listed as follows: CD45-147Sm, CD3e-152Sm, CD4-172Yb, CD8a-168Er, and IFNγ-165Ho (Fluidigm).

IHC staining of human breast tumor tissue samples

IHC staining was performed as described previously (19). Human breast tumor tissue specimens were obtained following the guidelines approved by the Institutional Review Board at MD Anderson Cancer Center, and written informed consent was obtained from patients in all cases. Briefly, tissue specimens were incubated with antibodies against PAR (Enzo Life Sciences, Clone 10H, 1:200 dilution) and PD-L1 (Abcam, Clone 288, #ab205921, 1:100 dilution) and a biotin-conjugated secondary antibody and then incubated with an avidin–biotin–peroxidase complex. Visualization was performed using amino-ethylcarbazole chromogen. According to the histologic scores, the intensity of staining was ranked into four groups: high (+++), medium (++), low (+), and negative (–).

Statistical analysis

Statistical analyses were performed using GraphPad Prism software (GraphPad). Student *t* test or one-way ANOVA was used

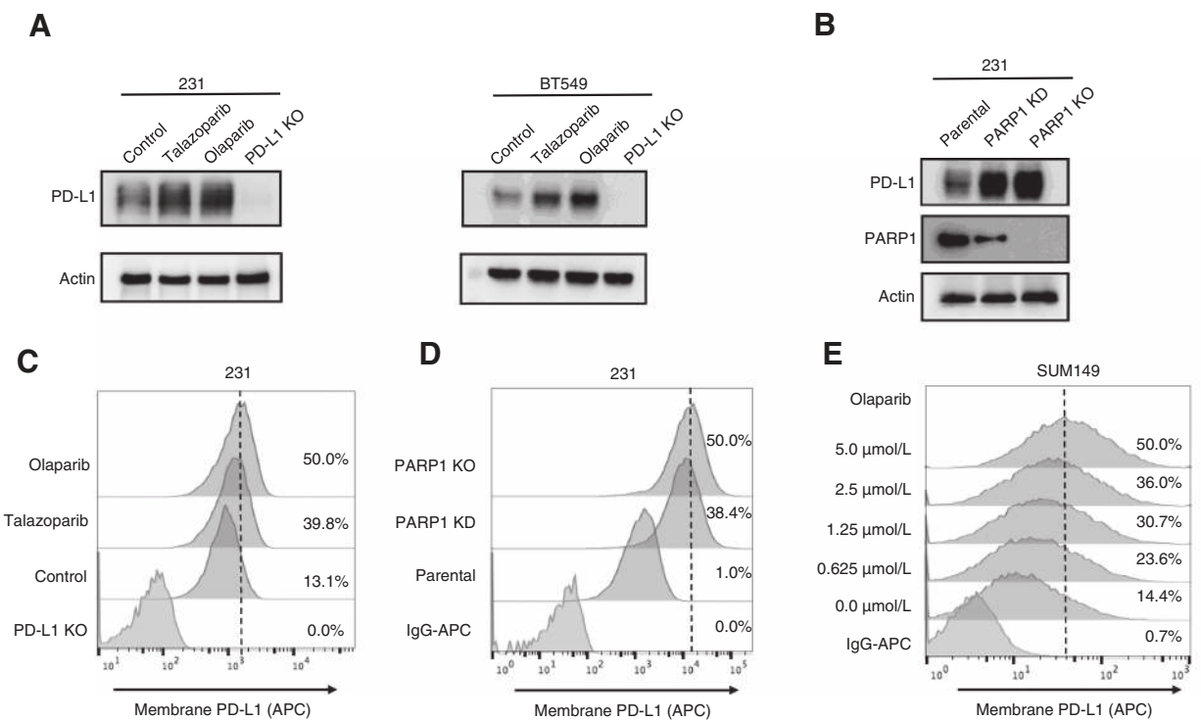

Figure 1.

PARPi upregulates PD-L1 protein expression in breast cancer cells. **A,** MDA-MDA-MB-231 and BT549 cells were treated with 10 μmol/L olaparib or 10 nmol/L talazoparib for 24 hours and subjected to immunoblotting with the indicated antibodies. PD-L1 KO cells were included as a negative control. **B,** PD-L1 expression in PARP1 KD, PARP1 KO, and MDA-MB-231 parental cells by immunoblotting. **C** and **D,** The indicated MDA-MB-231 cells were subjected to FACS analysis for cell surface PD-L1 expression. **E,** SUM149 cells were treated with the indicated concentrations of olaparib for 10 days, and cell surface PD-L1 expression was determined by FACS. APC, allophycocyanin.

to compare experimental data. The Pearson χ^2 test was used to analyze IHC data. A P value <0.05 (*) was considered statistically significant.

Results

PARPi enhances PD-L1 expression *in vitro* and *in vivo*

Elevated PD-L1 expression in cancer cells has been shown to enhance PD-L1/PD-1 axis–mediated anticancer immunosuppression (11, 16). To determine whether inhibition of PARP affects the PD-L1 protein level, we treated MDA-MB-231 and BT549 cells with two different PARPis, olaparib and talazoparib, and determined PD-L1 expression by immunoblotting. PARPi treatment increased the total level of PD-L1 protein in both the cell lines (Fig. 1A). To validate whether PARPi-induced PD-L1 upregulation is through PARP1 inhibition, we knocked down (KD) or knocked out (KO) PARP1 in MDA-MB-231 cells. Consistent with the results shown in Fig. 1A, PD-L1 expression in the PARP1 KD and KO cells was substantially higher compared with the parental cells (Fig. 1B).

PD-L1 expressed on cell surface of cancer cells exerts immunosuppressive effects by binding to PD-1 receptor on activated T cells (20). To determine whether the level of cell surface PD-L1 increases after PARPi treatment, MDA-MB-231 cells were treated with or without PARPi and subjected to FACS using fluorescence-labeled PD-L1 antibody. Cell surface PD-L1 levels significantly increased after olaparib and talazoparib treatment (Fig. 1C), and the increase occurred in a dose-dependent manner (Supplementary Fig. S1). Likewise, cell surface PD-L1 levels were higher in PARP1 KD and KO MDA-MB-231 cells than in parental cells (Fig. 1D). Because PARPi is commonly used to treat *BRCA*-deficient cancers (21), we also investigated the effects of olaparib on *BRCA*-mutant SUM149 cells. SUM149 cells were treated with the different concentrations of olaparib for 10 days to mimic chronic PARPi exposure in clinic and subjected to FACS to determine PD-L1 expression. Consistent with the results in MDA-MB-231 cells, cell surface PD-L1 was significantly increased following olaparib treatment in a dose-dependent manner (Fig. 1E). To further validate the role of *BRCA* deficiency in PARPi-induced PD-L1 upregulation, we knocked down *BRCA1* or *BRCA2* in MDA-MB-231 cells and exposed cells to olaparib. Downregulation of *BRCA1* or *BRCA2* had virtually no effect on PARPi-induced PD-L1 expression (Supplementary Fig. S2). These results together suggested that PARPi can upregulate cell surface PD-L1 level in both *BRCA*-proficient and *BRCA*-deficient cells.

Next, we asked whether PARPi may affect PD-L1 expression in tumors; we inoculated BT549 and SUM149 cells into the mammary fad pads of nude mice, and after the tumor formed, administered olaparib to mice 5 days a week for 3 weeks. Tumor tissues from xenografts were isolated and subjected to immunoblotting with PD-L1 antibody. As shown, PD-L1 expression was substantially higher in the xenograft tumors from mice treated with olaparib compared with those from the untreated mice (Fig. 2A and B). We also assessed PD-L1 expression by IHC staining in MDA-MB-231 xenograft tumor tissues from mice that had been treated with another PARPi, rucaparib, and harvested from our previous study (9). Mice treated with rucaparib for 3 weeks had higher PD-L1 expression in their tumors compared with control mice (Fig. 2C). Together, these

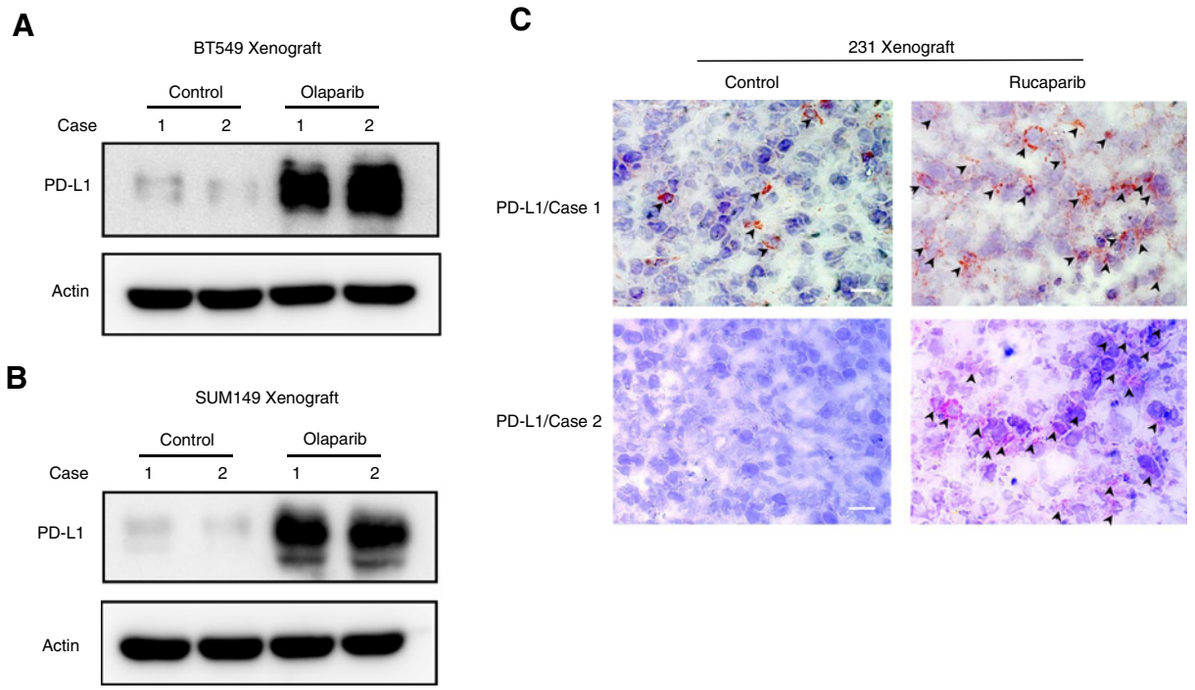

Figure 2.

PARPi upregulates PD-L1 expression in xenograft tumors. **A–C,** BT549 (**A**), SUM149 (**B**), and MDA-MB-231 cells (**C**) were inoculated into the mammary fad pad of nude mice, and the mice with established tumors were treated with olaparib or rucaparib. Tumors were then isolated to evaluate PD-L1 expression by immunoblotting (**A** and **B**) or IHC staining (**C**). Black arrowheads, detected PD-L1 signals. Scale bar, 50 μm.

results indicated that PARPi upregulates PD-L1 expression in triple-negative breast cancer *in vitro* and *in vivo*.

GSK3β inactivation is required for PARPi-induced PD-L1 upregulation

Next, we explored the mechanism underlying PARPi-enhanced PD-L1 protein expression. Multiple signaling pathways, such as STAT, NF-κB, and mTOR, have been reported to regulate PD-L1 expression level (19, 22, 23). In an attempt to identify the potential signaling pathways that regulate PD-L1, we performed a phospho-kinase antibody array screen to identify kinases that are activated or inactivated following PARPi treatment. In the presence of PARPi treatment, the phosphorylation signal of GSK3α/β at Ser21 and Ser9, which represents its inactivated form (24), scored the second highest after the CHK2-p53 DNA repair pathway (Fig. 3A). CHK2 kinase is known to respond to DNA damage, and PARPi-induced CHK2 phosphorylation has previously been reported (25, 26), further lending support to the results of our screen. The finding that PARPi inactivates GSK3α/β is also in line with our recent report demonstrating inactivation of GSK3β (p-Ser9) stabilizes PD-L1 (27). Those findings together prompted us to investigate whether PARPi upregulates the expression of PD-L1 via inactivation of GSK3β. To this end, we examined the status of GSK3β phosphorylation at Ser9 in response to PARPi in SUM149 cells, BT549, and MDA-MB-231 cells by immunoblotting. The results indicated that PARPi treatment induced high GSK3β Ser9 phosphorylation that was associated with PD-L1 upregulation (Fig. 3B and C; Supplementary Fig. S3). Knocking out GSK3β significantly increased PD-L1 expression (Fig. 3C, lane 3 vs. 1). However, PD-L1 expression level in GSK3β KO cells was no longer enhanced by olaparib treatment (Fig. 3C, lane 4 vs. 3). These results suggested that inactivation of GSK3β is required for the PARPi-induced PD-L1 upregulation.

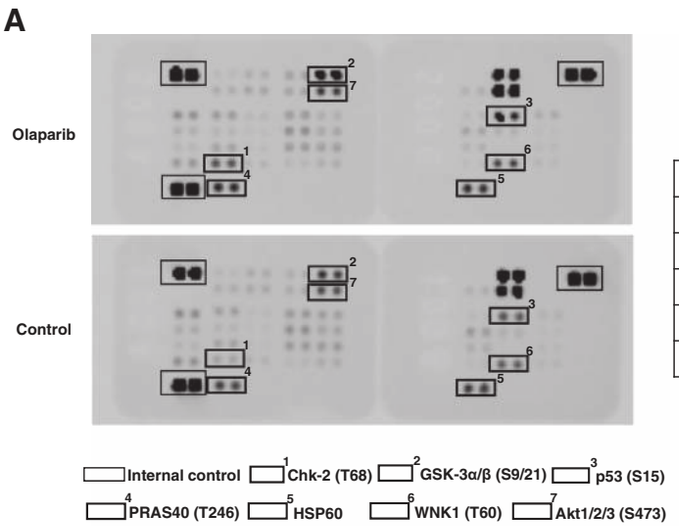

Top 5 Kinases/substrates responding to olaparib treatment identified by the human phospho-kinase array

Phosphorylation	Ratio (Olaparib/control)	Type
CHK2 (T68)	2.6	Kinase
GSK-3α/β (S9/21)	1.9	Kinase
p53 (S15)	1.5	Substrate
PRAS40 (T246)	1.2	Substrate
HSP60	1.1	Substrate

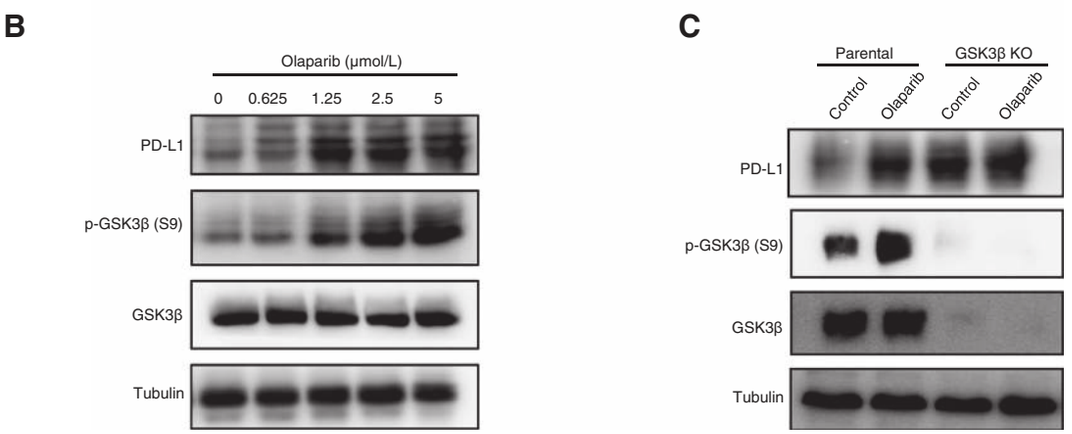

Figure 3.

GSK3β inactivation is required for PARPi-mediated PD-L1 upregulation. **A,** SUM149 cells were treated with olaparib and subjected to human phospho-kinase array. The top two responding kinases were Chk2 and GSK3α/β. **B,** SUM149 cells were treated with the indicated concentrations of olaparib for 10 days and subjected to immunoblotting with the indicated antibodies. **C,** BT549 parental or GSK3β KO cells were treated with 10 μmol/L olaparib for 24 hours. PD-L1 expression was evaluated by immunoblotting.

PARPi attenuates T-cell killing through PD-L1 induction

To understand the functional significance of PD-L1 upregulation by PARPi, we first asked whether PARPi-induced PD-L1 increases PD-1 binding on cells. Exposure of MDA-MB-231 cells to olaparib induced more PD-1 binding to PD-L1 on the cell surface (Fig. 4A). Similar results were observed in MDA-MB-231 PARP1 KD and KO cells (Fig. 4B), and in SUM149 cells treated with different concentrations of olaparib (Fig. 4C). Next, to

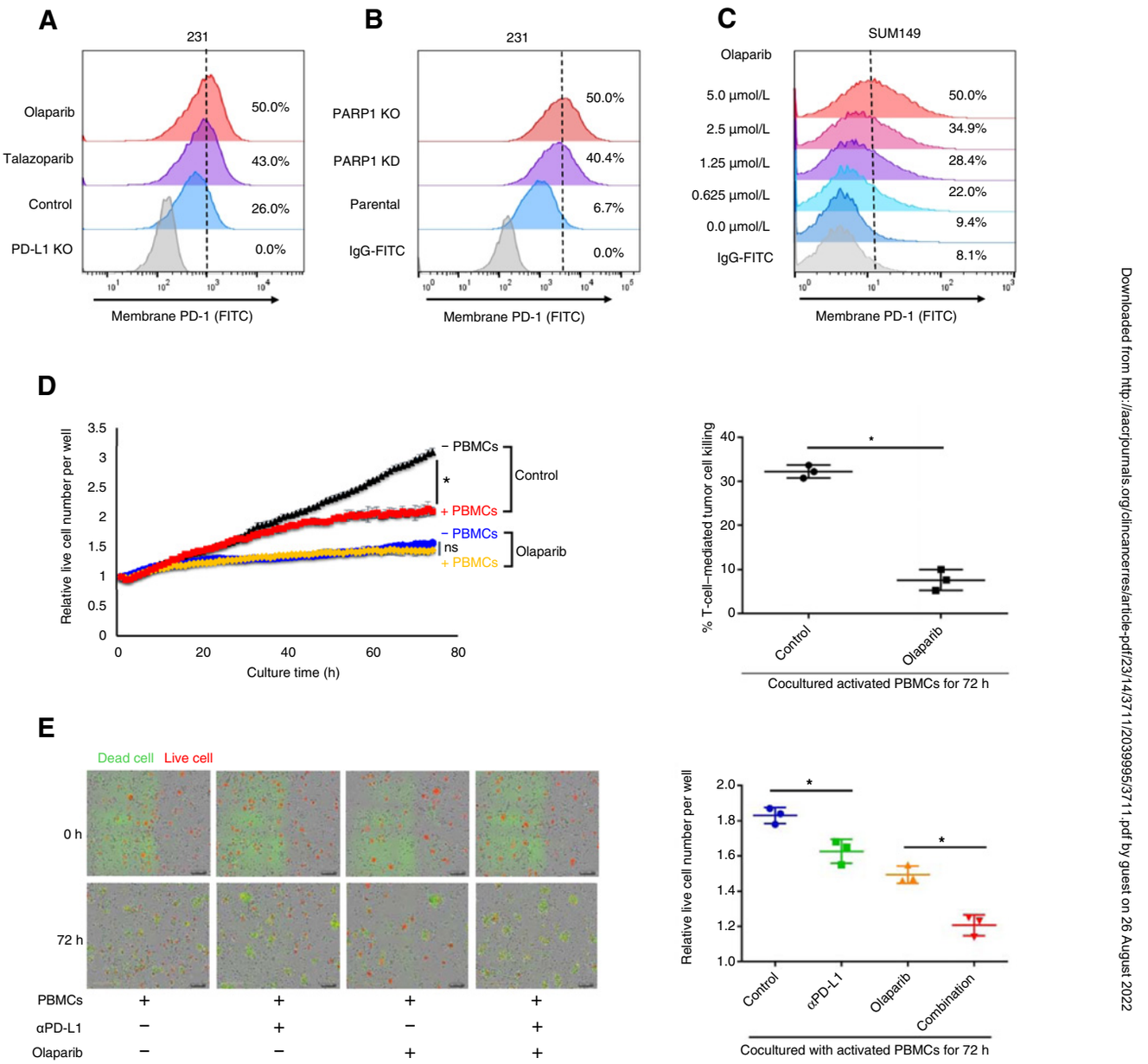

Figure 4.

Olaparib increases PD-1 binding and attenuates T-cell–mediated cell death in triple-negative breast cancer cells. **A,** FACS analysis of cell surface PD-1 binding of MDA-MB-231 cells treated with 10 μmol/L olaparib or 10 nmol/L talazoparib for 24 hours. **B,** FACS analysis of PARP1 KD, PARP1 KO, and parental MDA-MB-231 cells. **C,** SUM149 cells were treated with the indicated concentrations of olaparib for 10 days. **D,** MDA-MB-231 cells expressing nuclear RFP protein were first treated with or without olaparib (10 μmol/L) for 3 hours and then cocultured with or without activated PBMCs. Left, quantitation showing the number of live cells per well, counting the number of red fluorescent objects, normalized to that at the zero time point. Right, the percent of T-cell–meditated tumor cell killing observed at 72 hours in activated PBMC coculture with control or olaparib-treated cells (normalized to coculture without PBMCs). **E,** Left, representative merged images showing red fluorescent (nuclear restricted RFP) and green fluorescent (caspase-3/7 substrate) objects in MDA-MB-231 cells cocultured with activated PBMCs at 0 and 72 hours. Images were taken using the IncuCyte Zoom microscope. Right, quantitation showing the number of live cells following treatment with olaparib (10 μmol/L), PD-L1 antibody (PD-L1 Ab; 10 μg/mL), or the combination cocultured with activated PBMCs for 72 hours. The number of live cells (red fluorescent objects) were counted and normalized to that at the zero time point. *, $P < 0.05$. ns, not significant.

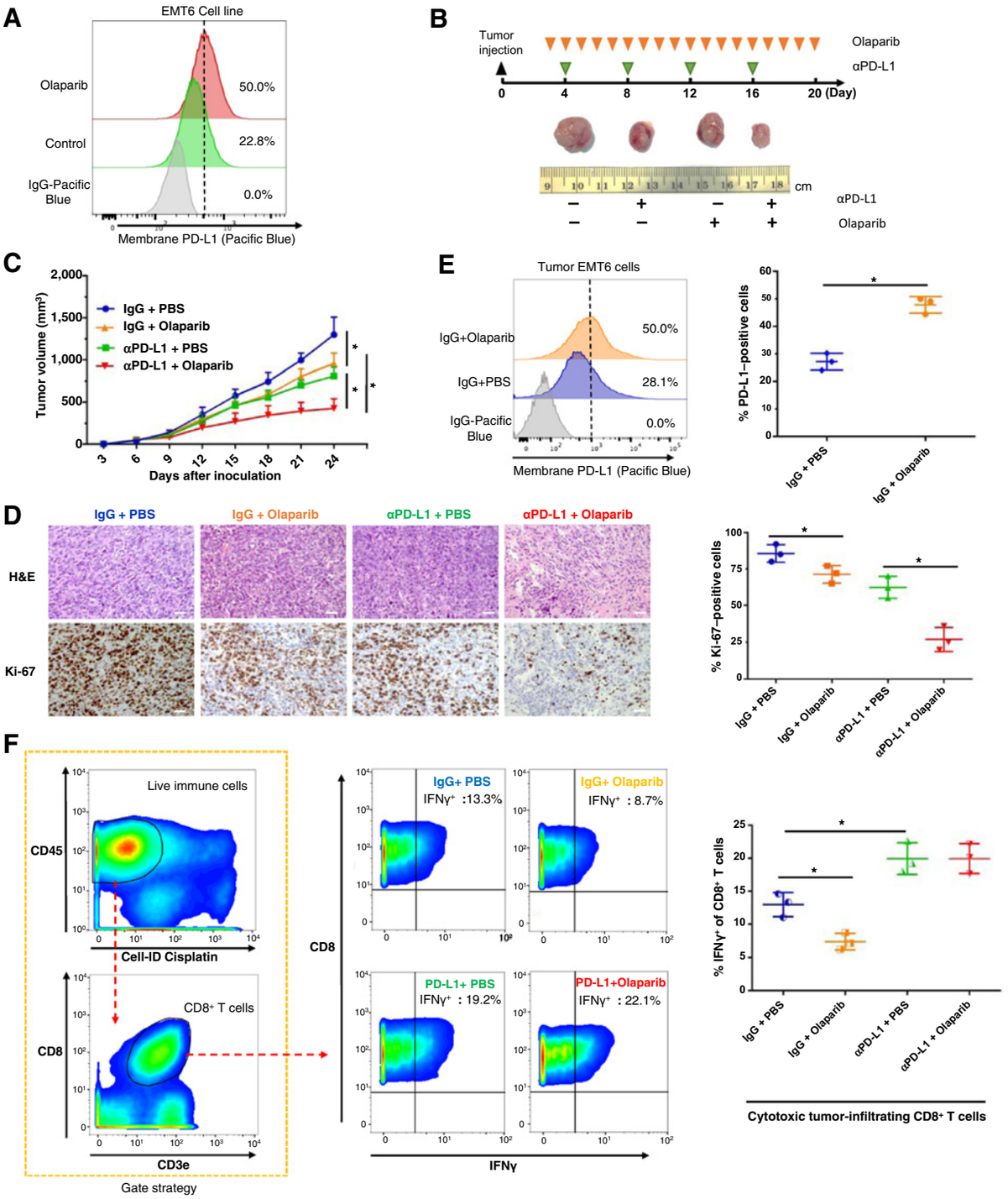

Figure 5.

PARPi-induced PD-L1 upregulation suppresses anticancer immunity, and blockade of PD-L1 potentiates PARPi. **A,** EMT6 cells were treated with 10 μmol/L olaparib for 24 hours. Cell surface PD-L1 were analyzed by FACS. **B,** Representative images of tumors after olaparib and/or anti-PD-L1 antibody treatment at the indicated time points in the EMT6 syngeneic mouse model. **C,** Effects of olaparib and/or anti-PD-L1 antibody treatment on tumor growth in EMT6 syngeneic mouse model treated ($n = 8$). Tumors were measured at the indicated time points and dissected for tumor cell PD-L1 expression analysis, TIL analysis, and pathologic analysis at the endpoint. **D,** Hematoxylin and eosin (H&E) and Ki-67 staining of EMT6 tumors. Scale bar, 50 μm. **E,** Cell surface PD-L1 expression in EMT6 cells derived from EMT6 mouse tumors. **F,** Cytotoxic $CD8^+$ T-cell population ($IFN\gamma^+$ $CD8^+$ $CD3^+$ $CD45^+$) in TILs isolated from EMT6 tumors by CyTOF analysis. *, $P < 0.05$.

determine whether PARPi-mediated PD-L1 upregulation, which resulted in increased PD-1 binding, affects T-cell function, we performed a T-cell–mediated killing assay by coculturing activated human PBMCs with MDA-MB-231 cells labeled with nuclear red fluorescence protein (RFP; NucLight Red MDA-MB-231) in the presence or absence of olaparib. As expected, olaparib efficiently inhibited cancer cell proliferation (black vs. blue in Fig. 4D, left; Supplementary Fig. S4A; Supplementary, Movie S1 vs. S2) but did not inhibit activated PBMC proliferation (Supplementary Fig. S4B). Interestingly, although MDA-MB-231 cells were sensitive to the T-cell killing (black vs. red in Fig. 4D, left; Supplementary Movie S3), those that were treated with olaparib were strongly resistant to activated T-cell killing (blue vs. yellow in Fig. 4D, left and right; Supplementary Movie S4), supporting the notion that upregulation of PD-L1 by PARPi may render the PARPi-treated cancer cells more resistant to T-cell killing. On the basis of the above results, we tested the T-cell killing effects of the combination of PD-L1 antibody and olaparib. The results showed that blockage of PD-L1 resensitized PARPi-treated MDA-MB-231 cells to activated T-cell killing and that the PARPi–PD-L1 antibody combination was more effective than each agent alone (Fig. 4E).

Combination with PD-L1 blockade sensitizes PARPi therapy

Next, we sought to determine whether PD-L1 blockade could further potentiate PARPi antitumor efficacy *in vivo*. We first treated a murine breast cancer cell line, EMT6, with olaparib with results showing significant induction of PD-L1 by olaparib (Fig. 5A). Consequently, we evaluated PARPi and anti-PD-L1 treatment alone or in combination in the EMT6 syngeneic mouse model. Consistent with our observations *in vitro*, both olaparib and anti-PD-L1 restricted tumor growth, but the

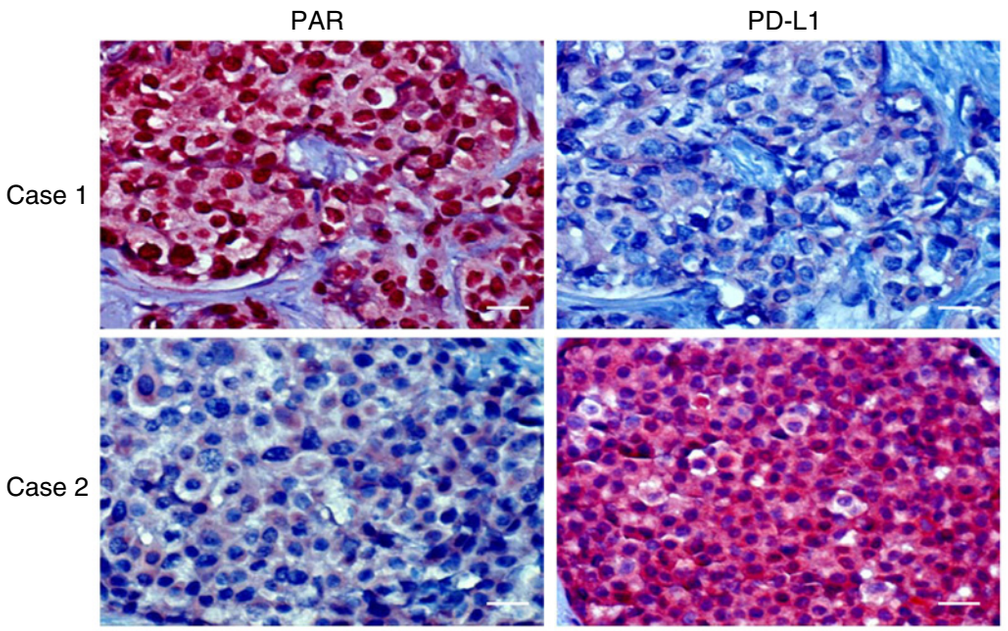

		PAR			
		–/+	++/+++	Total	*P* value
PD-L1	–/+	15 (12.9%)	65 (56.0%)	80 (69.0%)	
	++/+++	14 (12.1%)	22 (19.0%)	36 (31.0%)	
	Total	29 (25.0%)	87 (75.0%)	116 (100.0%)	$P = 0.02$

Figure 6.

Inverse correlation between PAR and PD-L1 in surgical specimens of breast cancer. Top, representative images of IHC staining of PAR and PD-L1 in human breast cancer tissues ($n = 116$). Scale bar, 50 μm; bottom, correlation analysis between PAR and PD-L1 was analyzed using the Pearson χ^2 test ($P = 0.02$). A P value of less than 0.05 was considered to be statistically significant.

combined treatment demonstrated better therapeutic benefit than each treatment alone (Fig. 5B and C). There were significantly fewer Ki-67–positive tumor cells in the combined treatment compared with each treatment alone (Fig. 5D). Mice that received the combination treatment did not show any significant changes in body weight or elevation in liver enzyme (ALT and AST), and kidney toxicity marker, blood urea nitrogen (Supplementary Fig. S5). At the end of the treatment, tumors resected from mice were subjected to dissociation, and tumor cells and TILs were separately harvested. Consistent with the observation in xenograft mouse model (Fig. 2), PARPi significantly upregulated PD-L1 expression on tumor cell surface as determined by FACS in EMT6 syngeneic mice (Fig. 5E). Analysis of TILs by CyTOF showed that tumor-infiltrating cytotoxic $CD8^+$ T-cell population, as measured by the level of IFNγ, decreased after PARPi treatment. Meanwhile, the addition of anti-PD-L1 restored the cytotoxic $CD8^+$ T-cell population (Fig. 5F). These results suggested that PARPi enhances cancer-associated immunosuppression through upregulation of PD-L1 and that PD-L1 blockade potentiates PARPi therapy.

Correlations of PARylation and PD-L1 expression in human tumor tissues

PARP exerts its biological function through its PARylation enzyme activity, and PARP inhibitors are designed to inhibit its enzyme activity. Thus, the extent of protein PARylation was utilized to assess the efficacy of PARP inhibition (7). To further validate our findings in human cancer patient samples, we analyzed the correlations between PARylation level and PD-L1 expression in human breast tumor specimens using IHC. High level of protein PARylation was detected in 87 (75.0%) of the 116 specimens, of which 65 cases (74.7%) showed low PD-L1 expression (Fig. 6, top). The Pearson χ^2 test further showed the inverse correlation between PARylation level and PD-L1 expression exists in human cancer patient specimens (Fig. 6, bottom). These results supported the notion that high PARP enzyme activity suppresses PD-L1 expression.

Discussion

Although the cytotoxic effects of PARPi have been well studied, the role of PARP inhibition in cancer-associated immunity is still largely unknown. In this study, we demonstrated that PARPi upregulates PD-L1 expression primarily through GSK3β inactivation. PARPi renders cancer cells more resistant to T-cell–mediated cell death, and PD-L1 blockade potentiates PARPi *in vitro* and *in vivo*. These data strongly suggested that PD-L1 upregulation by PARPi treatment attenuates PARPi therapeutic efficacy via tumor-associated immunosuppression, and simultaneous inhibition of PARP and PD-L1 may benefit breast cancer patients. There are currently three clinical trials testing the combination of PARPi (olaparib, niraparib, and BGB-290) and PD-L1 or PD-1 antibody in multiple cancer types (NCT02484404, NCT02657889, NCT02660034). The results of the current study provided scientific basis for these clinical trials.

Higuchi and colleagues recently investigated the combination of PARPi and CTLA4 antibody in the BR5-AKT ovarian cancer syngeneic mouse model and claimed to have observed a synergistic therapeutic effect (28); however, they indicated they did not observe such synergistic effect using the anti-PD-1 and PARPi combination in the same animal model. It is worthwhile to mention that PD-1 blockade in the BR5-AKT syngeneic mice did not affect T-cell activation or cytokine induction in the peritoneal tumor environment in their study (28), and therefore, synergistic effects may not be observed in combination with PARPi under their experimental condition. Moreover, because BR5-AKT tumors display high AKT activities that already inhibit GSK3β (29), it is possible that PARPi cannot further inhibit GSK3β and upregulate PD-L1 in the BR5-AKT tumors, and thus, the synergistic effects were not observed. In contrast, the results from our study indicated that PARPi upregulates PD-L1 in EMT6 tumors and PD-L1 blockade attenuated immunosuppression activity (Fig. 5F), which allowed us to observe an anti-PD-L1 therapy–potentiated antitumor activity of PARPi. Meanwhile, other studies have reported that chemotherapeutic agents, gemcitabine and paclitaxel, can induce PD-L1 in ovarian cancer cells (30, 31). The combination of paclitaxel and PD-L1/PD-1 blockade enhanced antitumor efficacy in an ID8 ovarian syngeneic mouse model (30). Therefore, whether the combination of PD-L1 blockade and PARPi induces synergistic effect in ovarian cancer warrants further investigation in a suitable animal model. Nonetheless, the mechanism of interaction between PARP and PD-L1/PD-1 as shown in the current study is timely and provides scientific basis to develop more effective combination therapies consisting of two powerful anticancer agents.

Disclosure of Potential Conflicts of Interest

J.K. Litton reports receiving commercial research grants from Genentech, Medivation, Novartis, and Pfizer, reports receiving speakers bureau honoraria from Medscape, and is a consultant/advisory board member for Medivation and Novartis. B. Arun is an employee of Abbvie. No potential conflicts of interest were disclosed by the other authors.

Authors' Contributions

Conception and design: S. Jiao, M.-C. Hung

Development of methodology: S. Jiao, H.-H. Lee, C.-W. Li, S.-O. Lim

Acquisition of data (provided animals, acquired and managed patients, provided facilities, etc.): S. Jiao, W. Xia, H. Yamaguchi, Y. Wei, M.-K. Chen, C.-K. Chou, B. Arun, G.N. Hortobagyi

Analysis and interpretation of data (e.g., statistical analysis, biostatistics, computational analysis): S. Jiao, W. Xia, M.-K. Chen, J.-M. Hsu, C.-W. Li, J. Litton, B. Arun, G.N. Hortobagyi, M.-C. Hung

Writing, review, and/or revision of the manuscript: S. Jiao, H. Yamaguchi, J.-L. Hsu, J. Litton, B. Arun, G.N. Hortobagyi, M.-C. Hung

Administrative, technical, or material support (i.e., reporting or organizing data, constructing databases): S. Jiao, J.-M. Hsu, W.-H. Yu, Y. Du, H.-H. Lee, S.-S. Chang, G.N. Hortobagyi

Study supervision: G.N. Hortobagyi, M.-C. Hung

Grant Support

This work was partially supported by the following: the NIH (CCSG CA016672), Cancer Prevention & Research Institutes of Texas (DP150052 and RP160710), Breast Cancer Research Foundation grant (to M.-C. Hung and G.N. Hortobagyi), Patel Memorial Breast Cancer Endowment Fund, National Breast Cancer Foundation, Inc., The University of Texas MD Anderson Cancer Center-China Medical University and Hospital Sister Institution Fund (to M.-C. Hung), Ministry of Science and Technology, International Research-intensive Centers of Excellence in Taiwan (I-RiCE; MOST 105-2911-I-002-302), and Ministry of Health and Welfare, China Medical University Hospital Cancer Research Center of Excellence (MOHW106-TDU-B-212-144003).

Received December 21, 2016; revised January 25, 2017; accepted January 28, 2017; published OnlineFirst February 6, 2017.

References

1. Sonnenblick A, de Azambuja E, Azim HA Jr, Piccart M. An update on PARP inhibitors–moving to the adjuvant setting. Nat Rev Clin Oncol 2015; 12:27–41.
2. Kim G, Ison G, McKee AE, Zhang H, Tang S, Gwise T, et al. FDA approval summary: olaparib monotherapy in patients with deleterious germline BRCA-mutated advanced ovarian cancer treated with three or more lines of chemotherapy. Clin Cancer Res 2015;21:4257–61.
3. Mirza MR, Monk BJ, Herrstedt J, Oza AM, Mahner S, Redondo A, et al. Niraparib maintenance therapy in platinum-sensitive, recurrent ovarian cancer. N Engl J Med 2016;375:2154–64.
4. Ibrahim YH, García-García C, Serra V, He L, Torres-Lockhart K, Prat A, et al. PI3K inhibition impairs BRCA1/2 expression and sensitizes BRCA-proficient triple-negative breast cancer to PARP inhibition. Cancer Discov 2012;2:1036–47.
5. Juvekar A, Burga LN, Hu H, Lunsford EP, Ibrahim YH, Balmañà J, et al. Combining a PI3K inhibitor with a PARP inhibitor provides an effective therapy for BRCA1-related breast cancer. Cancer Discov 2012;2:1048–63.
6. Karnak D, Engelke CG, Parsels LA, Kausar T, Wei D, Robertson JR, et al. Combined inhibition of Wee1 and PARP1/2 for radiosensitization in pancreatic cancer. Clin Cancer Res 2014;20:5085–96.
7. Kummar S, Chen A, Ji J, Zhang Y, Reid JM, Ames M, et al. Phase I study of PARP inhibitor ABT-888 in combination with topotecan in adults with refractory solid tumors and lymphomas. Cancer Res 2011;71:5626–34.
8. Muvarak NE, Chowdhury K, Xia L, Robert C, Choi EY, Cai Y, et al. Enhancing the cytotoxic effects of PARP Inhibitors with DNA demethylating agents - a potential therapy for cancer. Cancer Cell 2016;30:637–50.
9. Du Y, Yamaguchi H, Wei Y, Hsu JL, Wang HL, Hsu YH, et al. Blocking c-Met-mediated PARP1 phosphorylation enhances anti-tumor effects of PARP inhibitors. Nat Med 2016;22:194–201.
10. Freeman GJ, Long AJ, Iwai Y, Bourque K, Chernova T, Nishimura H, et al. Engagement of the PD-1 immunoinhibitory receptor by a novel B7 family member leads to negative regulation of lymphocyte activation. J Exp Med 2000;192:1027–34.
11. Dong H, Strome SE, Salomao DR, Tamura H, Hirano F, Flies DB, et al. Tumor-associated B7-H1 promotes T-cell apoptosis: a potential mechanism of immune evasion. Nat Med 2002;8:793–800.
12. Hodi FS, O'Day SJ, McDermott DF, Weber RW, Sosman JA, Haanen JB, et al. Improved survival with ipilimumab in patients with metastatic melanoma. N Engl J Med 2010;363:711–23.
13. Robert C, Long GV, Brady B, Dutriaux C, Maio M, Mortier L, et al. Nivolumab in previously untreated melanoma without BRAF mutation. N Engl J Med 2015;372:320–30.
14. Garon EB, Rizvi NA, Hui R, Leighl N, Balmanoukian AS, Paul Eder J, et al. Pembrolizumab for the treatment of non-small-cell lung cancer. N Engl J Med 2015;372:2018–28.
15. Rosenberg JE, Hoffman-Censits J, Powles T, van der Heijden MS, Balar AV, Necchi A, et al. Atezolizumab in patients with locally advanced and metastatic urothelial carcinoma who have progressed following treatment with platinum-based chemotherapy: a single-arm, multicentre, phase 2 trial. Lancet 2016;387:1909–20.
16. Reck M, Rodríguez-Abreu D, Robinson AG, Hui R, Csőszi T, Fülöp A, et al. Pembrolizumab versus chemotherapy for PD-L1-positive non-small-cell lung cancer. N Engl J Med 2016;375:1823–33.
17. Galluzzi L, Buqué A, Kepp O, Zitvogel L, Kroemer G, et al. Immunological effects of conventional chemotherapy and targeted anticancer agents. Cancer Cell 2015;28:690–714.
18. Xia W, Chen JS, Zhou X, Sun PR, Lee DF, Liao Y, et al. Phosphorylation/cytoplasmic localization of p21Cip1/WAF1 is associated with HER2/neu overexpression and provides a novel combination predictor for poor prognosis in breast cancer patients. Clin Cancer Res 2004;10: 3815–24.
19. Lim SO, Li CW, Xia W, Cha JH, Chan LC, Wu Y, et al. Deubiquitination and stabilization of PD-L1 by CSN5. Cancer Cell 2016;30:925–39.
20. Topalian SL, Drake CG, Pardoll DM. Targeting the PD-1/B7-H1(PD-L1) pathway to activate anti-tumor immunity. Curr Opin Immunol 2012; 24:207–12.
21. Kaufman B, Shapira-Frommer R, Schmutzler RK, Audeh MW, Friedlander M, Balmaña J, et al. Olaparib monotherapy in patients with advanced cancer and a germline BRCA1/2 mutation. J Clin Oncol 2015;33:244–50.
22. Bellucci R, Martin A, Bommarito D, Wang KS, Freeman GJ, Ritz J, et al. JAK1 and JAK2 modulate tumor cell susceptibility to natural killer (NK) cells through regulation of PDL1 expression. Blood 2013;122:3472.
23. Parsa AT, Waldron JS, Panner A, Crane CA, Parney IF, Barry JJ, et al. Loss of tumor suppressor PTEN function increases B7-H1 expression and immunoresistance in glioma. Nat Med 2007;13:84–8.
24. Cohen P, Frame S. The renaissance of GSK3. Nat Rev Mol Cell Biol 2001;2:769–76.
25. Hirao A, Kong YY, Matsuoka S, Wakeham A, Ruland J, Yoshida H, et al. DNA damage-induced activation of p53 by the checkpoint kinase Chk2. Science 2000;287:1824–7.
26. Anderson VE, Walton MI, Eve PD, Boxall KJ, Antoni L, Caldwell JJ, et al. CCT241533 is a potent and selective inhibitor of CHK2 that potentiates the cytotoxicity of PARP inhibitors. Cancer Res 2011;71:463–72.
27. Li CW, Lim SO, Xia W, Lee HH, Li CC, Kuo CW, et al. Glycosylation and stabilization of programmed death ligand-1 suppresses T-cell activity. Nat Commun 2016;7:12632.
28. Higuchi T, Flies DB, Marjon NA, Mantia-Smaldone G, Ronner L, Gimotty PA, et al. CTLA-4 blockade synergizes therapeutically with PARP Inhibition in BRCA1-deficient ovarian cancer. Cancer Immunol Res 2015;3:1257–68.
29. Xing DY, Orsulic S. A mouse model for the molecular characterization of Brca1-associated ovarian carcinoma. Cancer Res 2006;66:8949–53.
30. Peng J, Hamanishi J, Matsumura N, Abiko K, Murat K, Baba T, et al. Chemotherapy induces programmed cell death-ligand 1 overexpression via the nuclear factor-κB to foster an immunosuppressive tumor microenvironment in ovarian cancer. Cancer Res 2015;75:5034–45.
31. Ding ZC, Lu X, Yu M, Lemos H, Huang L, Chandler P, et al. Immunosuppressive myeloid cells induced by chemotherapy attenuate antitumor CD4 (+) T-cell responses through the PD-1-PD-L1 axis. Cancer Res 2014;74: 3441–53.